

Exclusive C–C Activation in the Rhodium(I) PCN Pincer Complex. A Computational Study

Andreas Sundermann, Olivier Uzan, and Jan M. L. Martin*

Department of Organic Chemistry, Kimmelman Building, Room 262, Weizmann Institute of Science, IL-76100 Rehovot, Israel

Received February 2, 2001

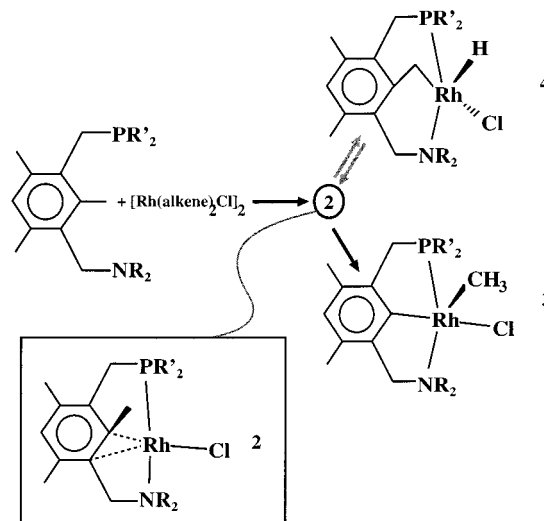
The mechanism of competitive intramolecular C–C and C–H bond activation in PCN pincer complexes of rhodium(I) has been studied computationally. Experimentally this system exhibits exclusive cleavage of an aryl–methyl C–C bond; no products corresponding to C–H bond cleavage in the methyl group have been observed. The calculated relative energies indicate that the C–C activation product is the most stable one ($\Delta E < -50 \text{ kJ}\cdot\text{mol}^{-1}$ relative to the C–H activation product) and that its formation is irreversible. C–H activation is not kinetically forbidden, but it is fast and reversible. Because of the weak Rh–N bond several intermediates on the C–H activation paths are accessible; therefore low concentrations of these species are a plausible reason for the experimental result. Further, this study reveals that the unique preference of C–C bond activation in the PCN system results from insufficient stabilization of the C–H activation product due to strain. To model the complete ligand including all bulky substituents used in the experiment, the ONIOM method has been employed, using the B3LYP/lanl2dz level for the inner layer and the HF/lanl1mb level to model substituent effects.

1. Introduction

Transition metal complexes are well known to cleave nonactivated C–H bonds under mild conditions.^{1–6} Using PCP type pincer ligands, Milstein et al. showed that intramolecular C–C bond activation may occur on the same time scale,^{7–9} although the corresponding activation barriers are usually considered to be much higher.^{10,11}

For the PCP system the reaction mechanism involves an intermediate structure from which both C–C and C–H activation are possible. Experimental investigations^{7–9} supported by quantum chemical calculations^{12,13} give evidence that in the case of $M = \text{Rh}$ the C–C activation product is thermodynamically more stable than the C–H activation product. The latter can slowly interconvert to the former, but C–H and C–C bond activation could be observed simultaneously.

Scheme 1



* Corresponding author. E-mail: comartin@wicc.weizmann.ac.il.

- (1) Bergman, R. G. *Science* **1984**, *223*, 902–908.
- (2) Crabtree, R. H. *Chem. Rev.* **1985**, *85*, 245–269.
- (3) Crabtree, R. H. In *The Chemistry of Alkanes and Cycloalkanes*; Patai, S., Rappoport, Z., Eds.; Wiley: New York, 1992.
- (4) Burger, P.; Bergman, R. G. *J. Am. Chem. Soc.* **1993**, *115*, 10462–10463.
- (5) Arndtsen, B. A.; Bergman, R. G.; Mobley, T. A.; Peterson, T. H. *Acc. Chem. Res.* **1995**, *28*, 154–167.
- (6) Niu, S.; Hall, M. B. *Chem. Rev.* **2000**, *100*, 353–406.
- (7) Gozin, M.; Weisman, A.; Ben-David, Y.; Milstein, D. *Nature* **1993**, *364*, 699–701.
- (8) Liou, S.-Y.; Gozin, M.; Milstein, D. *J. Am. Chem. Soc.* **1995**, *117*, 9774–9775.
- (9) Rybtchinski, B.; Vigalok, A.; Ben-David, Y.; Milstein, D. *J. Am. Chem. Soc.* **1996**, *118*, 12406–12415.
- (10) Sakaki, S.; Mizoe, N.; Musashi, Y.; Biswas, B.; Sugimoto, M. *J. Phys. Chem. A* **1998**, *102*, 8027–8036.
- (11) Koga, N.; Morokuma, K. *J. Am. Chem. Soc.* **1993**, *115*, 6883–6892.
- (12) Sundermann, A.; Uzan, O.; Milstein, D.; Martin, J. M. L. *J. Am. Chem. Soc.* **2000**, *122*, 7095–7104.
- (13) Cao, Z.; Hall, M. B. *Organometallics* **2000**, *19*, 3338–3346.

For the PCN ligand (i.e., a system in which one phosphino group is replaced by an amino group, see Scheme 1) the experiment reveals no C–H activation at all by rhodium(I).¹⁴ This outcome is surprising, since C–H bond activation of saturated hydrocarbons is usually expected to be kinetically as well as thermodynamically favored.^{15,16} To rationalize the high selectivity of the PCN/rhodium(I) system toward C–C bond activation, two explanations could be considered.¹⁴

(14) Gandelman, M.; Vigalok, A.; Shimon, L. J. W.; Milstein, D. *Organometallics* **1997**, *16*, 3981–3986.

(15) Rybtchinski, B.; Milstein, D. *Angew. Chem., Int. Ed.* **1999**, *38*, 871–883.

(16) Blomberg, M. R. A.; Siegbahn, P. E. M.; Nagashima, U.; Wennenberg, J. *J. Am. Chem. Soc.* **1991**, *113*, 424–433.

1. C–C activation is kinetically favored; oxidative addition to the C–H bond is therefore suppressed, and the system selectively cleaves the carbon–carbon bond.

2. The C–C product is thermodynamically more stable, while C–H activation (though taking place) is very fast and reversible. In this case the C–H product presumably could not be detected in the experiment (i.e., by NMR spectroscopy) because of its short lifetime and/or low concentration.

The application of quantum chemical methods promises to make a decision possible. In this computational study we aimed to locate relevant stationary points on the energy hypersurface to uncover potential steps of the reaction mechanism because several intermediates are hidden to the experimental approach due to their elusive character.

In comparison with the PCP/rhodium(I) system, a further complication in the reaction mechanism results from the difference in bond strengths between the Rh–P and the Rh–N bond. The more labile coordination of the hard amine donor¹⁷ could allow the corresponding “arm” of the chelating ligand to detach during or prior to the activation reaction. This change in the coordination number of the rhodium atom may open an alternative reaction pathway with different relative activation energies for C–C and C–H bond cleavage. So we had to extend our search to areas of the energy hypersurface involving “open” structures, i.e., structures with the PCN “pincers” acting as a monodentate ligand.

2. Computational Methods

The PCN ligand possesses no symmetry, so a complete DFT (density functional theory) optimization of several stationary points (transition states and minima) with even a double- ζ basis set is not feasible for the ligand used in the experiment. Unfortunately, the bulky substituents cannot be neglected (as we showed for the PCP ligand system in a recent paper¹²), so we employed the ONIOM approach developed by Morokuma et al.¹⁸ to model the complete ligand system with all substituents used in the experiment (i.e., the ligand 1-((diethylamino)methyl)-3-((di-*tert*-butylphosphino)methyl)-2,4,6-trimethylbenzene).

We defined a two-layer model. The outer layer comprises the entire complex, and the inner layer consists of the “generic” complex (i.e., the ligand 1-(aminomethyl)-3-(phosphinomethyl)-benzene; all bulky substituents at the nitrogen and phosphorus atoms as well as the two methyl groups in 4 and 6 position of the phenyl ring are replaced by hydrogens).

Relativistic corrections to the electronic energy are included implicitly for both layers by the use of relativistic effective core potentials (RECPs). The inner layer is described at the B3LYP density functional level¹⁹ with a basis set of valence double- ζ quality (lanl2dz basis set/RECP^{20–22}), whereas for the outer layer the Hartree–Fock/minimal basis set level was utilized (lanl1mb basis set/RECP^{20–22}). We will abbreviate this combination as “ONIOM(B3LYP/lanl2dz:HF/lanl1mb)”. For the parameter “*f*” of the ONIOM method the default values of the implementation in the Gaussian 98 set of programs²³ have been used (i.e., *f* = 0.773169 for P–C, 0.723886 for C–C, and 0.700189 for N–C bonds).²⁴ This parameter defines the posi-

Table 1. Structural Parameters for Structures 3 (Bond Lengths in Å, Angles in deg)

	R				
	H ^a	methyl ^a	methyl ^b	full ^b	expt ¹⁴
RhC _{ipso}	1.999	1.989	1.994	2.008	1.970(4)
RhC	2.057	2.055	2.055	2.046	2.044(4)
RhN	2.119	2.184	2.207	2.260	2.186(3)
RhP	2.354	2.339	2.299	2.354	2.2307(11)
RhCl	2.499	2.532	2.527	2.546	2.4576(10)
∠NRhP	165.2	164.4	163.9	161.2	160.16(10)
∠C _{ipso} RhCl	166.6	165.4	165.1	174.6	170.04(11)
∠CRhC _{ipso}	90.8	88.1	88.0	85.9	80.9(2)

^a B3LYP/lanl2dz. ^b ONIOM(B3LYP/lanl2dz:HF/lanl1mb).

tion of auxiliary hydrogen atoms that are needed to “saturate” the bonds cleaved for the inner layer calculation. “*f*” determines a fraction of the corresponding bond length. All molecular structures were completely optimized either at the B3LYP/lanl2dz or at the ONIOM(B3LYP/lanl2dz:HF/lanl1mb) level, using analytical gradients. The stationary points were characterized by inspection of the analytically calculated Hessians. The eigenvalues of the Hessian have also been used to estimate $\Delta G(298\text{ K})$ and $\Delta H(298\text{ K})$ within the rigid rotor/harmonic oscillator approximation.

In addition, single-point energy calculations at the B3LYP/lanl2dz+p or the ONIOM (B3LYP/lanl2dz+p:B3LYP/lanl2dz) level have been performed for all stationary points in order to obtain more reliable thermochemical data. The basis set lanl2dz+p consists of the lanl2dz basis set augmented by d polarization functions on P and Cl and a single f function on Rh.^{25,26} For first-row atoms the standard Dunning–Hay D95V(p,d) basis set²⁷ was utilized.

For all calculations the Gaussian 98 set of programs²³ was used, running on the SGI Origin 2000 of the Faculty of Chemistry of the Weizmann Institute and on SGI Octane, Compaq XP 1000, and Compaq ES 40 workstations in our laboratory. The structures have been visualized using the program MOLDED 3.6.²⁸

3. Results and Discussion

3.1. Suitability of the ONIOM Model. For the C–C activation product (**3**) formed with the ligand 1-((diethylamino)methyl)-3-((di-*tert*-butylphosphino)methyl)-2,4,6-trimethylbenzene a crystal structure is available.

A comparison of our calculated results with the experimental data (see Table 1) shows them to be in good agreement. The effect of the bulky substituents

(23) Frisch, M. J.; Trucks, G. W.; Schlegel, H. B.; Scuseria, G. E.; Robb, M. A.; Cheeseman, J. R.; Zakrzewski, V. G.; Montgomery, J. A., Jr.; Stratmann, R. E.; Burant, J. C.; Dapprich, S.; Millam, J. M.; Daniels, A. D.; Kudin, K. N.; Strain, M. C.; Farkas, O.; Tomasi, J.; Barone, V.; Cossi, M.; Cammi, R.; Mennucci, B.; Pomelli, C.; Adamo, C.; Clifford, S.; Ochterski, J.; Petersson, G. A.; Ayala, P. Y.; Cui, Q.; Morokuma, K.; Malick, D. K.; Rabuck, A. D.; Raghavachari, K.; Foresman, J. B.; Cioslowski, J.; Ortiz, J. V.; Stefanov, B. B.; Liu, G.; Liashenko, A.; Piskorz, P.; Komaromi, I.; Gomperts, R.; Martin, R. L.; Fox, D. J.; Keith, T.; Al-Laham, M. A.; Peng, C. Y.; Nanayakkara, A.; Gonzalez, C.; Challacombe, M.; Gill, P. M. W.; Johnson, B.; Chen, W.; Wong, M. W.; Andres, J. L.; Gonzalez, C.; Head-Gordon, M.; Replogle, E. S.; Pople, J. A. *GAUSSIAN 98, Revision A.7*; Gaussian, Inc.: Pittsburgh, PA, 1998.

(24) Dapprich, S.; Komáromi, I.; Byun, K. S.; Morokuma, K.; Frisch, M. J. *J. Mol. Struct.: THEOCHEM* **1999**, *461–462*, 1–21.

(25) Höllwarth, A.; Böhme, M.; Dapprich, S.; Ehlers, A. W.; Gobbi, A.; Jonas, V.; Köhler, K. F.; Stegmann, R.; Veldkamp, A.; Frenking, G. *Chem. Phys. Lett.* **1993**, *208*, 237–240.

(26) Ehlers, A. W.; Böhme, M.; Dapprich, S.; Gobbi, A.; Höllwarth, A.; Jonas, V.; Köhler, K. F.; Stegmann, R.; Veldkamp, A.; Frenking, G. *Chem. Phys. Lett.* **1993**, *208*, 111–114.

(27) Dunning, T. H., Jr.; Hay, P. J. In *Modern Theoretical Chemistry*; Schaeffer, H. F., III, Ed.; Plenum: New York, 1976.

(28) Schaftenaar, G. Molden 3.6, 1999. URL: <http://www.cmbi.kun.nl/~schaft/molten/molden.html>.

(17) Togni, A.; Venanzi, L. M. *Angew. Chem., Int. Ed.* **1994**, *33*, 497–526.

(18) Svensson, M.; Humbel, S.; Froese, R. D. J.; Matsubara, T.; Sieber, S.; Morokuma, K. *J. Phys. Chem.* **1996**, *100*, 19357–19363.

(19) Becke, A. D. *J. Chem. Phys.* **1993**, *98*, 5648–5653.

(20) Hay, P. J.; Wadt, W. R. *J. Chem. Phys.* **1985**, *82*, 270–283.

(21) Wadt, W. R.; Hay, P. J. *J. Chem. Phys.* **1985**, *82*, 284–298.

(22) Hay, P. J.; Wadt, W. R. *J. Chem. Phys.* **1985**, *82*, 299–310.

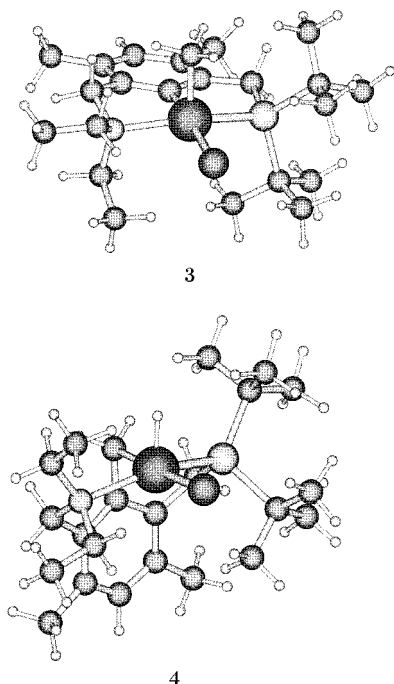


Figure 1. Perspective view of the C–C product **3** and the C–H product **4**. All substituents are shown in order to illustrate steric crowding.

Table 2. Structural Parameters for Structures 4 (Bond Lengths in Å, Angles in deg)

	R			
	H ^a	methyl ^a	methyl ^b	full ^b
RhH	1.534	1.532	1.534	1.524
RhC	2.106	2.109	2.119	2.099
RhN	2.150	2.261	2.299	2.383
RhP	2.375	2.363	2.313	2.362
RhCl	2.489	2.507	2.501	2.526
∠RhCC _{ipso}	84.5	84.8	84.7	88.7
∠NRhP	163.0	162.6	162.1	158.1
∠CRhCl	164.8	174.2	175.2	175.8
∠HRhC	90.3	90.3	90.8	87.8

^a B3LYP/lanl2dz. ^b ONIOM(B3LYP/lanl2dz:HF/lanl1mb).

(see Figure 1 for a perspective view) appears to be rather small in this structure, and even a calculation with hydrogen atoms replacing the bulky groups seems to reproduce the structural features of the ligand core quite well.

Unfortunately, the effect is more pronounced, for example, for the corresponding C–H activation product. Some calculated structural parameters for this complex (no experimental data are available) are given in Table 2.

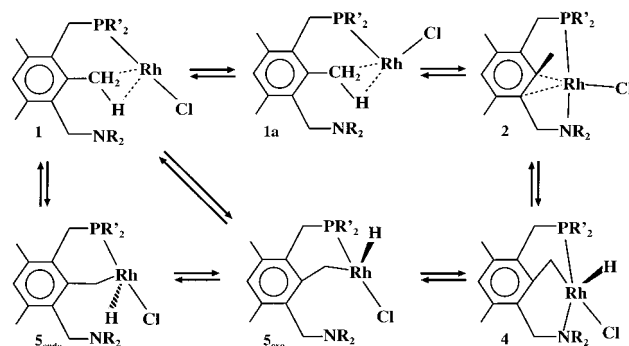
By the repulsive interaction of the rhodium-bound chlorine and the substituents of the phosphino and amino groups, especially the rhodium–nitrogen bond becomes longer ($\Delta r = 0.23$ Å relative to a system with hydrogen substituents). This might be interpreted as an indicator for the destabilizing effect of the bulky groups operative in this complex. As a consequence, substituent effects cannot be neglected, because the potential energy surface is distorted in favor of the C–C activation product due to this repulsive interaction ($\Delta E_{\text{CH-CC}} = 23.4$ kJ·mol⁻¹ for H, 39.2 kJ·mol⁻¹ for methyl, and 52.2 kJ·mol⁻¹ for the complete ligand (see Table 3)). We previously reported this finding for the PCP ligand system.¹²

Table 3. Comparison of ONIOM and DFT Energetic Data (in kJ·mol⁻¹)^c at Different Levels of Theory

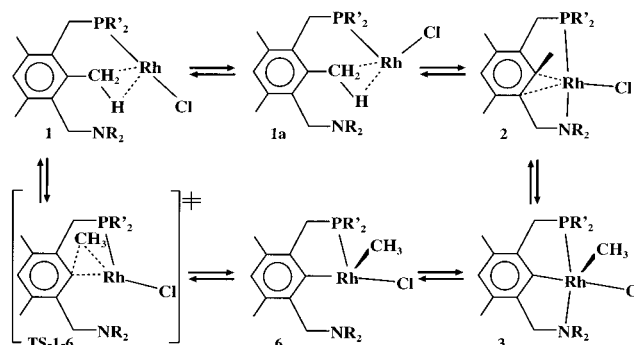
structure		H (DFT)	methyl (DFT)	methyl (ONIOM)	complete (ONIOM)
3	<i>a</i>	-45.5	-48.1	-47.9	-58.9
	<i>b</i>	-30.6	-34.0	-36.9	-52.1
4	<i>a</i>	-5.3	6.3	2.7	-7.4
	<i>b</i>	-7.2	5.2	9.4	-0.1
TS-2-3	<i>a</i>	55.7	62.5	63.6	58.2
	<i>b</i>	59.1	65.5	64.3	61.2
TS-2-4	<i>a</i>	39.0	56.9	58.2	55.2
	<i>b</i>	27.8	47.7	54.1	54.3

^a B3LYP/lanl2dz and ONIOM(B3LYP/lanl2dz:HF/lanl1mb), respectively. ^b B3LYP/lanl2dz+p/B3LYP/lanl2dz and ONIOM(B3LYP/lanl2dz+p:B3LYP/lanl2dz)/ONIOM(B3LYP/lanl2dz:HF/lanl1mb), respectively. ^c All energies are given relative to **2**.

Scheme 2



Scheme 3



For a complex with methyl substituents at the phosphorus and nitrogen atoms, both ONIOM and B3LYP/lanl2dz calculations for the entire molecule are feasible. These demonstrate that the error introduced by the low-level treatment of the outer layer is rather small. The bond lengths computed at both levels of theory suggest that the ONIOM calculation underestimates the Rh–P and overestimates the Rh–N distance relative to the DFT calculation by ≈ 0.04 Å. Since the deviations in the relative energies are smaller than 7 kJ·mol⁻¹ (see Table 4 for the relative energies) and the calculated harmonic frequencies for the Rh–N and Rh–P stretching modes differ by no more than 10 cm⁻¹ between both methods, we can assume that the error introduced by the approximations within the ONIOM method will not distort the energy profiles relative to a DFT treatment of the entire molecule, and we can rely on the error compensation.

3.2. Pathway Involving a Chelating PCN Ligand.

To find the reason for the high selectivity of the PCN system toward C–C cleavage (and decide which of our

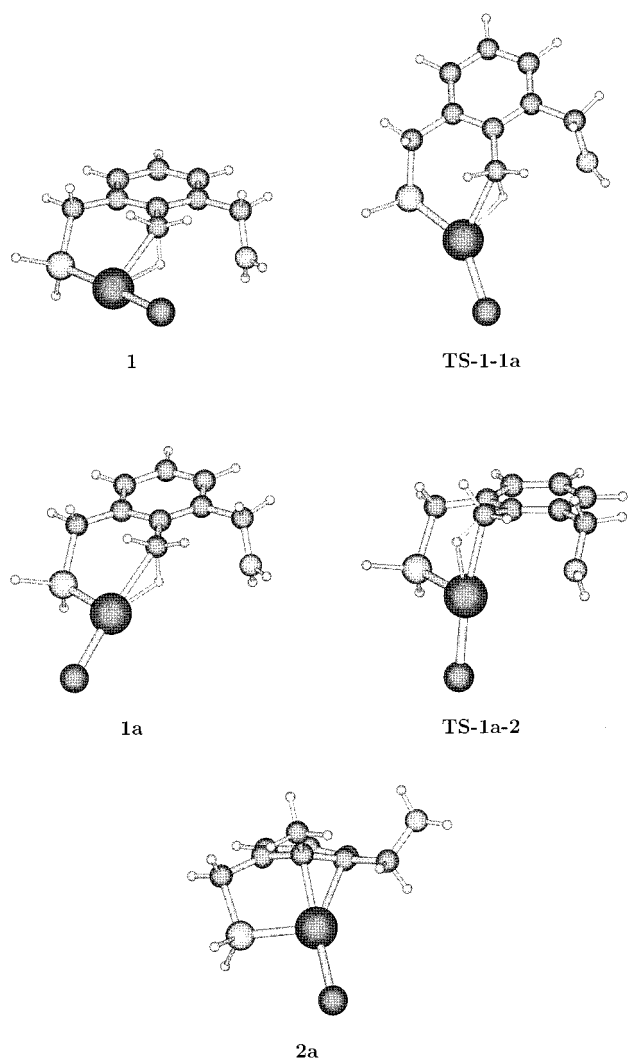
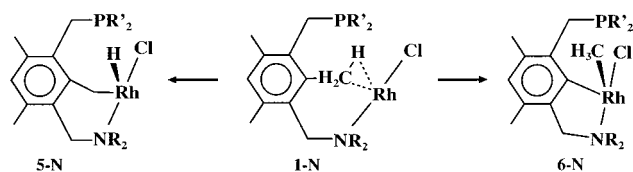


Figure 2. Perspective view of the stationary points involved in the conversion of the entry channel **1** to the η^2 intermediate **2**. Additionally, the alternative conformer **2a** is shown. The structures are optimized at the ONIOM-(B3LYP/lanl2dz:HF/lanl1mb) level. For clarity, in this and the following figures, all substituents have been replaced by hydrogen atoms (i.e., only the inner layer of the ONIOM calculation is shown). The Cartesian coordinates of all atoms are available as Supporting Information.

Scheme 4



two basic assumptions holds true), we explored a variety of reaction pathways (see Schemes 2–4). Starting from the coordinatively highly unsaturated rhodium(I) complex **1** (see Figure 2 for a perspective representation), several intramolecular reactions can occur.

In **1** a linearly coordinated rhodium(I) center forms an agostic bond with a C–H bond of the methyl group. We chose **1** as a possible entry channel for the activation reaction because it seems to be easily accessible by dissociation of a chloro-bridged dimer (see Figure 3), which is a plausible intermediate under the reaction

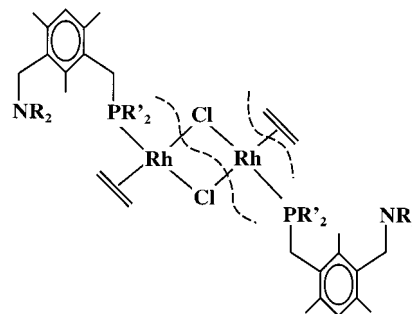


Figure 3. Schematic representation of a hypothetical dimeric intermediate formed from $[\text{Rh}(\text{C}_2\text{H}_4)_2\text{Cl}]_2$ and the PCN ligand. Calculations at the B3LYP/lanl2dz level for a model compound for this dimer ($[\text{Rh}(\text{C}_2\text{H}_4)(\text{PH}_3)\text{Cl}]_2$) reveal that the Rh–Cl bonds are cleaved in the way shown if the Rh–Rh distances are increased.

conditions present in the experiment.¹⁴ The reaction starts from a dimeric, chloro-bridged rhodium(I) olefin complex.^{29,30} Prior to the bond activation reaction a ligand substitution has to take place. Monodentate phosphine coordination seems to be the most plausible reaction at this stage.

According to our calculated energies (See Table 4), the most facile reaction pathway (i.e., the one with the lowest activation barrier) involves a conformational change from a linear to a bent arrangement of the phosphino and the chloro ligand bringing the agostic bond into the *trans* position of the chloro ligand. This step requires almost no activation energy ($\Delta E \approx 1 \text{ kJ}\cdot\text{mol}^{-1}$) and stabilizes the system by $44.5 \text{ kJ}\cdot\text{mol}^{-1}$. For comparison, we optimized the linear and the bent conformation of the dicoordinate rhodium(I) model complex $\text{RhCl}(\text{PH}_3)_2$. At the B3LYP/lanl2dz+p//B3LYP/lanl2dz level, the bent conformer was found to be $32.2 \text{ kJ}\cdot\text{mol}^{-1}$ more stable than the linear one. Thus, the influence of the agostic bond on the conformation preferred is rather small.

In the bent complex **1a**, the free coordination site of the unsaturated complex fragment is in an appropriate position to allow amino group attachment to form a square-planar ligand field (see Figure 2). For the Rh–N bond formation, the methyl group has to reorient, necessitating cleavage of the agostic bond. This causes an activation barrier of $11.2 \text{ kJ}\cdot\text{mol}^{-1}$ for the formation of **2**. Here, one coordination site in the square-planar ligand field of the rhodium atom is saturated by η^2 complex formation with the π system of the phenyl ring. Due to the increase in the coordination number from three to four, the complex is stabilized by $55.7 \text{ kJ}\cdot\text{mol}^{-1}$ (in comparison with **1a**).

The local minimum **2** is a common intermediate from which C–H as well as C–C activation is possible as depicted in Figure 4. Similar to the PCP system, both reactions are competitive and occur on the same time scale (our calculated activation energies are almost equal, $\Delta E \approx 60 \text{ kJ}\cdot\text{mol}^{-1}$). In contrast to the PCP ligand, no intermediate with a tetracoordinate rhodium atom and an agostic interaction with a C–H bond of the methyl group could be found here. The reason for this has to be sought not so much in electronic effects (e.g.,

(29) Cramer, R. *Inorg. Chem.* **1962**, *1*, 722.

(30) Herde, J. L.; Senoff, C. V. *Inorg. Nucl. Chem. Lett.* **1971**, *7*, 1029–1031.

Table 4. Relative Energies (in kJ·mol⁻¹)^a for All Stationary Points of the Rhodium(I) PCN Complex (PCN = 1-((Diethylamino)methyl)-3-((di-*tert*-butylphosphino)methyl)-2,4,6-trimethylbenzene) Calculated in This Study

structure	ΔE^b	ΔE^c	$\Delta G(298\text{ K})^b$	$\Delta H(298\text{ K})^b$
1	0	0	0	0
1(rot)	6.4	-4.0	3.6	6.4
TS-1-1a	10.8	1.1	12.7	8.1
1a	-26.7	-44.5	-21.2	-24.6
TS-1a-2	-1.8	-33.3	5.7	-3.0
2	-77.5	-100.2	-64.5	-74.6
2a	-0.6	-27.7	-0.1	1.2
3	-136.4	-152.3	-128.9	-141.1
TS-2-3	-19.3	-39.0	-7.7	-23.0
4	-84.9	-100.3	-69.6	-88.8
TS-2-4	-22.3	-45.9	-11.1	-30.9
5_{endo}(rot)	-70.5	-69.8	-87.4	-92.6
5_{endo}(rot)	-77.6	-83.3	-80.9	-83.5
5_{exo}(rot)	-64.9	-67.5	-67.3	-70.7
5_{exo}(rot)	-78.9	-82.6	-82.6	-84.8
TS-1-5_{endo}	14.5	6.5	8.7	4.1
TS-1-5_{exo}(rot)	35.3	28.7	28.0	25.1
TS-1-5_{exo}(rot)	35.6	16.8	28.6	26.4
TS-5_{endo}-5_{exo}	-40.3	-38.4	-39.8	-48.1
TS-4-5_{exo}	-59.2	-72.9	-59.5	-67.7
TS'-5_{endo}-5_{exo}	48.7	29.3	42.0	38.0
6	-70.6	-74.5	-80.4	-76.2
TS-1-6	51.9	29.6	45.0	43.5
7	-31.3	-67.0	-13.1	-25.1
TS-5_{endo}-7	-23.6	-40.6	-16.7	-33.8
1N	54.8	46.8	59.2	55.6
6N	-25.6	-22.4	-17.7	-25.5
5N	-13.6	-21.5	-9.5	-18.2
TS-1N-5N	68.4	54.8	67.1	59.0
TS-1N-6N	157.9	151.0	161.8	153.4
8	10.0	2.6	9.6	10.2
TS-8-9	22.8	9.4	16.2	12.7
9	-73.8	-76.7	-76.3	-79.3

^a The entry channel **1** was chosen as the origin of the energy scale. ^b ONIOM(B3LYP/lanl2dz:HF/lanl1mb). ^c ONIOM(B3LYP/lanl2dz+p:B3LYP/lanl2dz)//ONIOM(B3LYP/lanl2dz:HF/lanl1mb).

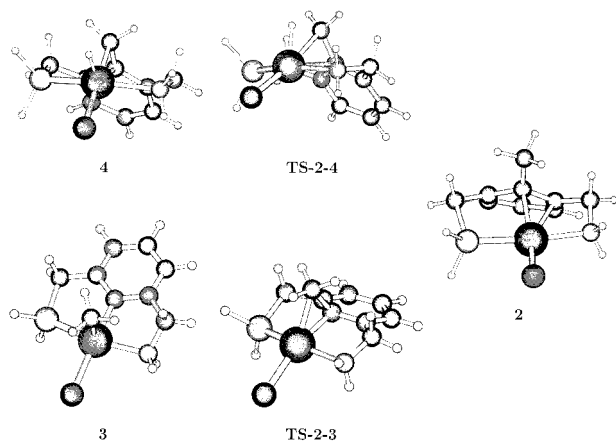


Figure 4. Perspective view of the stationary points involved in the interconversion of the C–H product into the C–C product: **4** → **TS-2-4** → **2** → **TS-2-3** → **3**. (For more details see caption of Figure 2.)

the amino group being a weaker donor) but predominantly in the fact that the amino “arm” is too short to allow an optimal interaction of the chelated rhodium atom with the C–H bonds of the methyl group. Because the C–N as well as the Rh–N bonds are shorter than the corresponding bonds in the phosphine “arm”, the rhodium atom is forced too close to the phenyl ring, and therefore the η^2 complex is favored. To demonstrate this,

we also optimized a conformation **2a** in which the “amino arm” is oriented *trans* to the phenyl ring (see Figure 4). For this minimum the Rh–C distances (Table 4) are very similar to those in **2**, but because of the missing stabilization by the amino coordination, **2a** is found to be 72.5 kJ·mol⁻¹ less stable than **2**. Its energy is very similar to the “open” agostic complex **1**. Thus, in the PCN system η^2 coordination and the formation of an agostic bond have comparable stabilizing effects on the transition metal atom, and the preference of the η^2 structure is a consequence of the binding to the amino “arm”.

Very recently, low-temperature observation of an intermediate for this reaction has been reported.³¹ Multinuclear NMR at -80 °C suggests a structure similar to **2** but lacking the η^2 (C_{ipso}–C_{ortho}) interaction. Experimental evidence appears to rule the latter out altogether. The reason for the discrepancy between computed and observed structures is not clear, but solvent effects would be a likely candidate.

The η^2 complex is connected on the energy hypersurface to the transition states for C–C (**TS-2-3**) and C–H activation (**TS-2-4**). For both reaction paths the amino and the phosphino groups remain bound to the rhodium atom throughout. The structures are qualitatively equivalent to the *C_s* symmetric ones found for the PCP ligand. The corresponding square-pyramidal product complexes are again similar to the structures found for the PCP ligand system: the basal positions are occupied by the donor atoms of the chelating “arms” and by the chloro ligand. In the apical position, either the methyl group (C–C product **3**) or the hydrogen atom (C–H product **4**) is found. A comparison of the relative energies reveals that **3** is by far the most stable structure we could find for the reaction system. It is by $\Delta E \approx 50$ kJ·mol⁻¹ more stable than the C–H product **4**. The latter has approximately the same energy as the η^2 complex **2**. This implies that C–H activation is reversible and the reductive elimination of C–H (i.e., the back-reaction of the activation) occurs at the same rate as the formation of **4**, while C–C activation is an irreversible process.

3.3. Pathway Involving only P-Coordination of the PCN Ligand. 3.3.1. C–H Activation. Starting from complex **1**, C–H and C–C activation should in principle be possible without attachment of the amino group.³² Therefore, we tried to locate the corresponding stationary points on the energy hypersurface.

Oxidative addition of the C–H bond to the rhodium atom is depicted in Scheme 2. For the C–H activation reaction via the transition state **TS-1-5_{endo}** only a very small activation energy of 6.5 kJ·mol⁻¹ is necessary. In the course of this reaction, the C–H product complex **5_{endo}** is formed; its structure is best described as a square-pyramidal complex fragment with one free coordination site in a basal position and the rhodium-bound hydrogen atom at the apex (for a perspective representation see Figure 5). In contrast to **4**, the latter is oriented *endo*, i.e., toward the phenyl ring of the ligand core.

(31) Gandelman, M.; Vigalok, A.; Konstantinovskii, L.; Milstein, D. *J. Am. Chem. Soc.* **2000**, *117*, 9848–9849.

(32) van der Boom, M. E.; Liou, S.-Y.; Shimon, L. J. W.; Ben-David, Y.; Milstein, D. *Organometallics* **1996**, *15*, 2562–2568.

Table 5. Selected Structural Parameters for the Stationary Points for the Complex with the Complete Ligand Included in This Study^a

structure	Rh–P	Rh–N	Rh–H/C	Rh–C	∠PRhCl/N	∠CRhH/C
1	2.342	4.605	1.861 ^H	2.456 ^m	174.0	26.8 ^H
1(rot)	2.346	5.622	1.821 ^H	2.489 ^m	174.8	25.7 ^H
TS-1-1a	2.302	4.587	1.843 ^H	2.488 ^m	146.0	26.0 ^H
1a	2.266	4.718	1.875 ^H	2.524 ^m	102.0	25.1 ^H
TS-1a-2	2.271	3.490	1.806 ^H	2.549 ^m	137.1	23.7 ^H
2	2.372	2.239	2.510 ^o	2.241 ⁱ	174.3 ^N	
2a	2.301	4.419	2.430 ^o	2.278 ⁱ	97.9	
3	2.354	2.260	2.046 ^m	2.008 ⁱ	161.2 ^N	88.5 ^C
TS-2-3	2.356	2.268	2.284 ^m	2.086 ⁱ	162.1 ^N	48.6 ^C
4	2.362	2.383	1.524 ^H	2.099 ^m	158.1 ^N	87.8 ^H
TS-2-4	2.369	2.302	1.593 ^H	2.214 ^m	159.4 ^N	42.9 ^H
5_{endo}	2.322	4.186	1.522 ^H	2.077 ^m	167.2	90.6 ^H
5_{endo}(rot)	2.339	5.065	1.519 ^H	2.068 ^m	173.0	92.9 ^H
5_{exo}	2.327	4.124	1.520 ^H	2.090 ^m	165.5	90.8 ^H
5_{exo}(rot)	2.348	4.903	1.522 ^H	2.065 ^m	174.8	92.1 ^H
TS-1-5_{endo}	2.333	4.345	1.604 ^H	2.222 ^m	171.6	39.7 ^H
TS-1-5_{exo}(rot)	2.319	4.735	1.594 ^H	2.166 ^m	173.7	42.5 ^H
TS-1-5_{exo}(rot)	2.345	4.849	1.612 ^H	2.288 ^m	176.1	34.2 ^H
TS-5_{endo}-5_{exo}	2.311	4.935	1.523 ^H	2.050 ^m	173.3	90.1 ^H
TS-4-5_{exo}	2.285	3.607	1.521 ^H	2.093 ^m	133.0	89.4 ^H
TS'-5_{endo}-5_{exo}	2.380	3.835	1.562 ^H	2.084 ^m	147.2	144.0 ^H
6	2.280	4.135	2.039 ^C	2.031 ^a	104.3	86.2 ^C
TS-1-6	2.287	4.079	2.285 ^C	2.121 ⁱ	98.7	47.7 ^C
7	2.290	3.805	2.833 ^H	2.066 ^m	176.6	2.164 [†]
TS-5_{endo}-7	2.364	3.134	1.831 ^H	2.052 ^m	159.8	77.3 ^H
1N	4.888	2.147	1.880 ^H	2.389 ^m	171.2 [*]	28.1 ^H
6N	3.696	2.153	2.042 ^C	1.993 ⁱ	166.1 [*]	93.6 ^C
5N	3.608	2.138	2.319 ^C	2.117 ⁱ	158.6 [*]	47.3
TS-1N-5N	4.362	2.171	1.519 ^H	2.047 ^m	166.8 [*]	87.8 ^H
TS-1N-6N	4.637	2.150	1.603 ^H	2.191 ^m	170.0 [*]	39.9 ^H
8	2.343		1.822 ^H	2.452 ^m	174.8	26.7 ^H
TS-8-9	2.339		1.596 ^H	2.221 ^m	173.8	39.2 ^H
9	2.341		1.522 ^H	2.341 ^m	172.0	91.7 ^H

^a Bond lengths in Å, angles in deg; ^Hreferring to rhodium bound hydrogen; ^Creferring to rhodium-bound methyl group; ^N∠PRhN instead of ∠PRhCl; ^{*}∠NRhCl; [†]bond length for the H–Cl hydrogen bond; ⁱ*ipso* carbon atom of the phenyl ring; ^mcarbon atom of the methyl group; ^o*ortho* carbon atom of the phenyl ring.

The formation of **5_{endo}** is an exothermic process; the reaction energy is $-69.8 \text{ kJ}\cdot\text{mol}^{-1}$. Thus, **5_{endo}** is only $30.5 \text{ kJ}\cdot\text{mol}^{-1}$ less stable than **4**. A direct conversion of **5_{endo}** into **4** by amino group attachment is not possible because a prior rotation from the *endo* to an *exo* orientation of the hydrogen atom is necessary. According to our calculations, this reaction is most likely to proceed via an intermediate **5_{exo}**, which differs only in the orientation of the rhodium-bound hydrogen. Consequently, both structures have almost equal energies (the energy difference of $2.2 \text{ kJ}\cdot\text{mol}^{-1}$ is below the accuracy of our method). The mechanism for the conversion of **5_{endo}** to **5_{exo}** involves the rotation of the rhodium-bound CH₂ group. The corresponding activation energy is $31.4 \text{ kJ}\cdot\text{mol}^{-1}$ (relative to **5_{endo}**). A direct rotation of the rhodium-bound hydrogen atom around the Cl–Rh–P axis with a planar-coordinated rhodium atom in the transition state **TS'-5_{endo}-5_{exo}** is symmetry forbidden and has an activation barrier of $99.1 \text{ kJ}\cdot\text{mol}^{-1}$.

In addition we also located a transition state for a direct formation of **5_{exo}** from **1**. This reaction proceeding via the transition state **TS-1-5_{exo}** requires an activation energy of $28.7 \text{ kJ}\cdot\text{mol}^{-1}$ because the rigidity of the phosphine arm does not allow an optimal Rh–C–H arrangement in the tricoordinate transition state. Therefore the route **1** → **5_{endo}** → **5_{exo}** seems to be more favorable.

Once the rhodium-bound hydrogen atom is in *exo* position, the amino “arm” can attach, saturating the free

coordination site in **5_{exo}**. The C–H activation product **4**, which is $32.9 \text{ kJ}\cdot\text{mol}^{-1}$ more stable than **5_{exo}**, is formed almost without barrier.

3.3.2. C–C Activation. We also investigated the oxidative addition of the C_{sp}²–C_{sp}³ bond to the rhodium atom involving the PCN ligand with a detached amino “arm”. The corresponding stationary points are depicted in Scheme 3.

To ensure that the amino group remains detached for all stationary points, we had to perform our calculations on a conformer with the amino group rotated by 120° around the N–C bond (for a pictorial representation of one of these structures see **5_{endo}(rot)** in Figure 4). Otherwise, the rhodium atom is always in such close proximity to the nitrogen lone pair that the amino group will attach without barrier and the “open” structures are not stationary points.

To ensure that the error introduced by this “trick” is small, we also calculated some stationary points from the “open” C–H activation reaction described above with the amino group in the rotated orientation. Accordingly, the stationary points with the amino group rotated are about $12\text{--}16 \text{ kJ}\cdot\text{mol}^{-1}$ more stable than the corresponding structures with the lone pair oriented toward the rhodium atom. Although these absolute numbers are not very meaningful, the important point is that the hypersurface is essentially parallel in both conformations, and therefore a comparison with the C–C activation reaction can be justified.

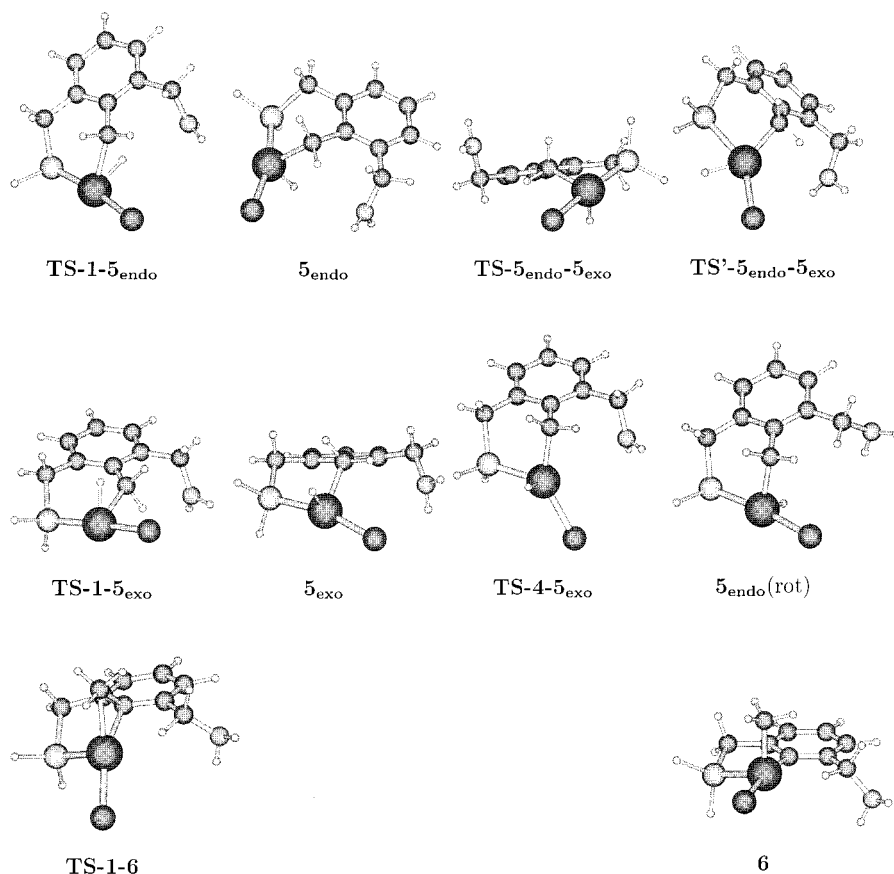


Figure 5. Perspective view of the stationary points involved in the C–H/C–C activation in the monodentate, P-coordinating PCN ligand. (For more details see caption of Figure 4.) Structure $5_{\text{endo}}(\text{rot})$ is an example of the conformers with a rotated amino group (as described in the text).

Our calculations reveal that the “open” C–C activation product **6** is *not* thermodynamically favored over the corresponding C–H activation product. **6** has about the same energy as 5_{endo} . Therefore, the high stability of the C–C product **3** over the corresponding C–H product stems from the stronger stabilization by the chelating amino “arm” and not from the formation of a strong Rh–C_{sp}² bond in the C–C product. The energy difference between **3** and **6** is 77.8 kJ·mol^{−1}. Nearly the same energy difference was found for **2** and **2a** (the η^2 complexes), while for the corresponding C–H products (**4** and 5_{endo}) only 32.8 kJ·mol^{−1} was calculated. This demonstrates that the PCN ligand is optimal in stabilizing the C–C activation product and fails for the stabilization of the C–H product.

An optimization of an open C–C activation transition state structure reveals that C–C activation without coordinating amino ligand has a higher barrier than C–H activation ($\Delta E = 74.1$ kJ·mol^{−1} relative to **1a**). This is in line with previous findings about C–C vs C–H activation by transition metal complexes.^{10,11,15,16} It further indicates that the high selectivity of the PCN system toward C–C bond activation has a thermodynamic origin. We could not find any reaction pathway involving a lower barrier for C–C than for C–H addition.

3.4. Pathway Involving Only N-Coordination of the PCN Ligand. For the sake of completeness, we also sought relevant stationary points involving the PCN ligand as a monodentate ligand binding with the amino group only. Because rhodium–nitrogen bonds are weaker

than rhodium–phosphorus bonds, the energies of these species are considerably higher than those for P-coordination. The N-coordinated agostic complex **1N** is 91.3 kJ·mol^{−1} less stable than **1**. Therefore, it is clear that this route is not competitive with those described above. However, the energies relative to **1N** are comparable to the corresponding energy differences found for the P-coordinated series (i.e., the activation energy for C–H addition is 13.6 kJ·mol^{−1} (6.5 kJ·mol^{−1} for P) and for C–C addition 104.2 kJ·mol^{−1} (74.1 kJ·mol^{−1} for P)), so we can rule out that selective C–C cleavage takes place via a route starting from an N-coordinated species, even if the system entered the reaction with a nitrogen-bound rhodium atom.

3.5. Rhodium–Nitrogen Proton Transfer. For the reaction of the PCN ligand with a platinum(II) complex, oxidative C–H addition followed by a proton transfer from the platinum atom to the amino group has been observed.¹⁴ Our calculations show that an intramolecular proton transfer is also possible in the rhodium system starting from structure 5_{endo} . In this complex, the detached amino group and the rhodium-bound hydrogen atom have the proper orientation to interact (see Figure 4). The proton transfer proceeds via a transition state with a linear Rh–H–N arrangement ($\angle \text{Rh–H–N} = 170^\circ$, see also Figure 4).

After the Rh–H bond is cleaved the resulting tautomer **7** is stabilized to some extent by an intramolecular hydrogen bond between the ammonium group and the rhodium-bound chlorine ($r(\text{H–Cl}) = 2.164$ Å; this hydrogen bond could also be observed in the X-ray

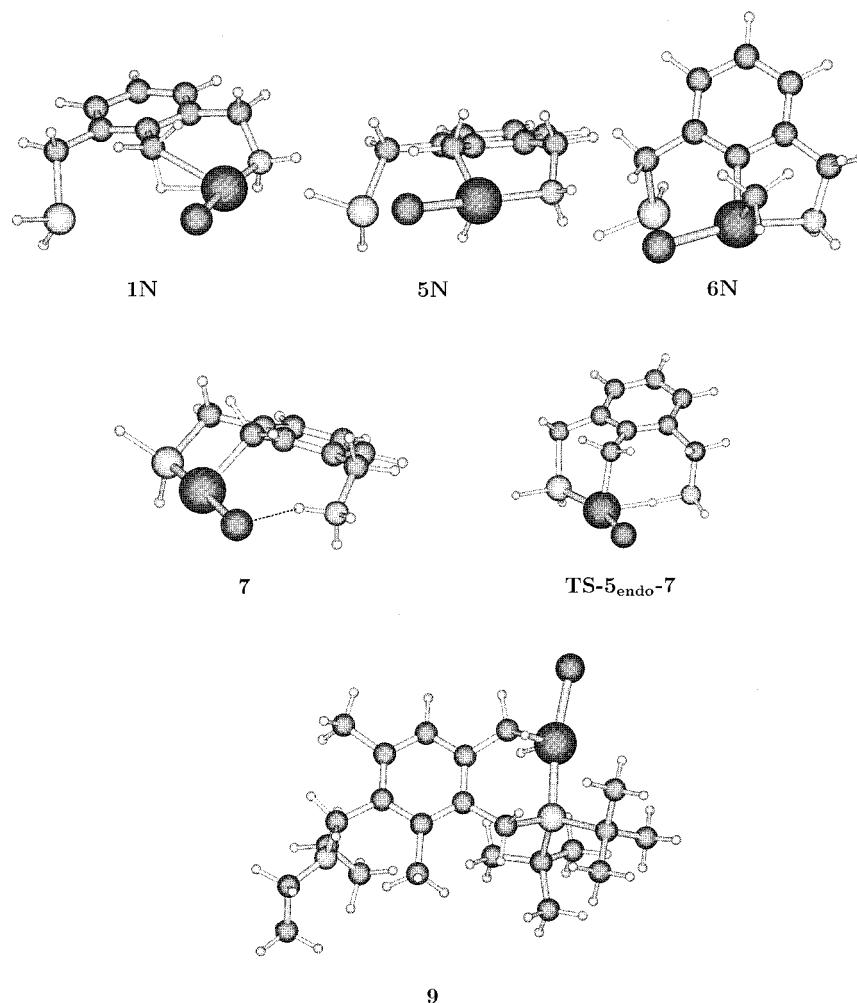
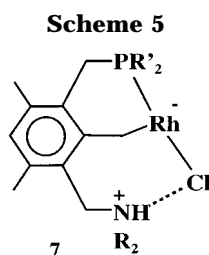


Figure 6. Perspective view of the stationary points relevant for an N-coordinated pathway, an intramolecular hydrogen transfer, and the activation of another aryl-methyl group (for **9** the complete complex is shown).



structure of the corresponding platinum compound), but it is still much less stable than the C–C product **3** ($\Delta E = 85.4 \text{ kJ}\cdot\text{mol}^{-1}$). Since **7** has about the same energy as the open C–H activation products **5_{endo}** and **5_{exo}** and an intramolecular proton transfer from **5_{endo}** is facile ($\Delta E^\ddagger = 29.6 \text{ kJ}\cdot\text{mol}^{-1}$ relative to **5_{endo}**), it can be assumed that reversible formation of **7** occurs during the reaction, **7** being completely converted into **3** because of the high stability of the latter.

3.6. Activation of Another Aryl-Methyl Group.

Experimentally, only activation of the methyl group located between the chelating arms (in 2 position of the phenyl ring) of the PCN ligand is observed.¹⁴ From a kinetic point of view, at least C–H bond cleavage cannot be excluded on the basis of our results given above, which demonstrate that intramolecular C–H bond cleavage does not require the attachment of the amino “arm” to the rhodium atom. In fact, our calculations

reveal that C–H activation of the other aryl-methyl group neighboring the phosphine “arm” has the same activation barrier—and gives a product of similar stability—as the reaction with the methyl group in 2 position yielding **5_{endo}**. This leads us to the assumption that activation (at least C–H activation) of other methyl groups takes place, but the corresponding products have no possibility for intramolecular stabilization by amino attachment. Therefore, these reactions are reversible and the complexes convert to the thermodynamically most stable complex, the C–C activation product **3**.

4. Conclusions

A computational study has been carried out on the mechanism of C–C and C–H activation by Rh(I) PCN pincer ligand systems. We may draw the following conclusions.

- The “closed” C–C activation product **3** is the most stable complex in the reaction system. It is formed irreversibly, while all other reactions we took into consideration seem to be reversible. Therefore, we assume that a variety of species (including products of C–H addition) are present in the reacting system. A facile interconversion of these is possible, and finally **3** is formed. Our calculations provide evidence that low concentration (we assume that the several C–H activated isomers are present during the reaction) and short

lifetimes are responsible for the “invisibility” of products other than **3** in the experiment.

- The calculations predict a common intermediate **2** with coordination of both the amino and phosphino group.

- C–H activation occurs at approximately the same rate as C–C activation if a reaction starting from **2** as a common intermediate is assumed. If the open agostic complex **1** is assumed as the entry channel, C–H activation is expected to be the faster reaction. The “closed” C–H activation product **4** is a strained molecule because the amino “arm” cannot bind optimally to the rhodium atom. This favors the stability of the C–C product and is the possible reason for the reversibility of the C–H bond cleavage, which is faster than in the PCP system.

- In the C–H activation product an intramolecular proton transfer from the rhodium atom to the nitrogen atom is possible, but the reaction is thermoneutral and reversible.

Acknowledgment. J.M. is a Yigal Allon Fellow and the incumbent of the Helen and Milton A. Kimmelman Career Development Chair. A.S. gratefully acknowledges a postdoctoral fellowship of the MINERVA Foundation, Munich, Germany. O.U. is a doctoral fellow of the Feinberg Graduate School, Weizmann Institute of Science. This research was supported by the MINERVA foundation, Munich, Germany, and by the Tashtiyot program of the Ministry of Science, Israel. The Compaq ES 40 server computer was jointly financed by the latter two programs. The authors would like to thank Prof. David Milstein (Weizmann Institute) for helpful discussions.

Supporting Information Available: Geometries in Cartesian coordinates and total energies for all species are available on the World Wide Web at the Uniform Resource Locator (URL) <http://theochem.weizmann.ac.il/web/papers/PCN-CCvsCH.html>. This material is also available free of charge via the Internet at <http://pubs.acs.org>.

OM0100838